

Article

Nuclear Data Sensitivity and Uncertainty Study for the Pressurized Water Reactor (PWR) Benchmark Using RMC and SCALE

Chengjian Jin ¹, Shichang Liu ^{1,*} , Shenghao Zhang ¹, Jingang Liang ²  and Yixue Chen ¹¹ School of Nuclear Science and Engineering, North China Electric Power University, Beijing 102206, China² Institute of Nuclear and New Energy Technology, Tsinghua University, Beijing 100084, China

* Correspondence: liu-sc@ncepu.edu.cn

Abstract: In order to improve the safety and economy of nuclear reactors, it is necessary to analyze the sensitivity and uncertainty (S/U) of the nuclear data. The capabilities of S/U analysis has been developed in the Reactor Monte Carlo code RMC, using the iterated fission probability (IFP) method and the superhistory method. In this paper, the S/U capabilities of RMC are applied to a typical PWR benchmark B&W's Core XI, and compared with the multigroup and continuous-energy S/U capabilities in the SCALE code system. The S/U results of the RMC-IFP method and the RMC-superhistory method are compared with TSUNAMI-CE/MG in SCALE. The sensitivity results and the uncertainty results of major nuclides that contribute a lot to the uncertainties in k_{eff} are in good agreement in both RMC and SCALE. The RMC-superhistory method has the same precision as the IFP method, but it reduces the memory footprint by more than 95% and only doubles the running time. The superhistory method has obvious advantages when there are many nuclides and reaction types to be analyzed. In addition, the total uncertainties in the k_{eff} of the first-order uncertainty quantification method are compared with the stochastic sampling method, and the maximum relative deviation of total uncertainties in the k_{eff} is 8.53%. Verification shows that the capabilities of S/U analysis developed in the RMC code has good accuracy.

Keywords: Monte Carlo; TSUNAMI-3D; SAMPLER; RMC; sensitivity and uncertainty

Citation: Jin, C.; Liu, S.; Zhang, S.; Liang, J.; Chen, Y. Nuclear Data Sensitivity and Uncertainty Study for the Pressurized Water Reactor (PWR) Benchmark Using RMC and SCALE. *Energies* **2022**, *15*, 9511. <https://doi.org/10.3390/en15249511>

Academic Editor: Guglielmo Lomonaco

Received: 11 October 2022

Accepted: 7 December 2022

Published: 15 December 2022

Publisher's Note: MDPI stays neutral with regard to jurisdictional claims in published maps and institutional affiliations.



Copyright: © 2022 by the authors. Licensee MDPI, Basel, Switzerland. This article is an open access article distributed under the terms and conditions of the Creative Commons Attribution (CC BY) license (<https://creativecommons.org/licenses/by/4.0/>).

1. Introduction

Neutron transport problem solution methods in reactor physical analysis can be divided into the deterministic method and the Monte Carlo (MC) method. Compared with the deterministic method, the Monte Carlo method has the advantages of fewer approximations to deal with three-dimensional complex geometric models and is suitable for complex geometric models. However, the calculation accuracy of the Monte Carlo is dependent on the number of simulated particles. In the early days, due to the high cost of computers, the Monte Carlo method was mainly used as a supplement to the deterministic method. With the development of computational tools, the Monte Carlo method is used more widely. Therefore, the validations and comparisons of the Monte Carlo codes are important.

A lot of research work has been carried out for the MC-based code-to-code and code-to-experiment validations and comparisons. D. Chersola compared Serpent 2 and MCNP6 for the evaluation of some important nuclear parameters in different positions of the LR-0 reactor mock-up [1]. Shichang Liu compared the deterministic codes DRAGON and DONJON with the Monte Carlo code RMC for the criticality and burnup-dependent neutronics of the JRR-3M plate-type research reactor [2,3]. Daniel J. Kelly III compared the MC21/CTF solution for VERA Core Physical Benchmark Progression problem 6 with the MC21/COBRA-IE and VERA solutions [4]. Jaakko Leppänen used the experimental

measurement results of the MIT BEAVRS benchmark for the validation of the Serpent-ARES code sequence [5].

At present, the codes with the capabilities of sensitivity and uncertainty analysis mainly include MCNP6 [6] developed by the Los Alamos National Laboratory in the United States, SCALE [7] developed by the Oak Ridge National Laboratory in the United States, MONK10 [8] developed by the Answering Software Center in the United Kingdom, and SERPENT2 [9] developed by the Finland National Technology Research Center, etc.

The reactor Monte Carlo analysis code RMC [10] developed by the Department of Engineering Physics of Tsinghua University is capable of handling complex geometric structures, describing complex spectra and materials using continuous-energy point cross-sections, calculating the eigenvalues and eigenfunctions of critical problems, on-the-fly cross-section treatment [11], and sensitivity and uncertainty analysis. The SCALE code system developed by the Oak Ridge National Laboratory [12] is widely used in criticality safety, reactor physics, shielding, sensitivity and uncertainty analysis. It is a modular code system in which the control module can call each function module in a specified order to accomplish a specific task.

Sensitivity analysis is a specified quantity describing the extent to which a change in a parameter affects the calculation results, as evaluated by the sensitivity coefficients [13]. By performing sensitivity analysis on each parameter of the system, important nuclear data (data with large sensitivity coefficients) can be obtained. In practical applications, the parameters that have the most effect on the output results can be separated from the many input parameters. This makes system analysis easier and makes sure that the output results are correct.

Uncertainty analysis methods mainly include the first-order uncertainty quantification method and the stochastic sampling method. The sensitivity coefficients are the basis of the first-order uncertainty quantification method [14]. In the Monte Carlo codes, solving the sensitivity coefficients has the problem of a large memory footprint, which is proportional to the number of particles simulated in each generation and the number of responses for sensitivity analysis [15,16]. Due to memory limitations, it is difficult to reduce the uncertainty of sensitivity statistics by increasing the number of particles. Uncertainty can be determined by the sandwich rule $r_y^2 = \vec{S} V_r \vec{S}^T$ [14]. This method depends on sensitivity coefficients. If the sensitivity coefficients can be calculated efficiently, the uncertainties of the responses caused by the uncertainties of each nuclear data can be given with this equation. The stochastic sampling method has a serious time-consuming problem. Generally, it can only analyze the total uncertainty of the calculation results caused by all the perturbed nuclear data at one time. If it is necessary to analyze the uncertainty of the calculation results caused by the uncertainty of each parameter in turn, each parameter should be perturbed and calculated separately.

The reactor physical design mostly adopts the best estimate technology, and its calculation results are affected by engineering uncertainties such as fuel manufacturing tolerance, calculation uncertainties such as calculation model approximation, and phenomenon uncertainties such as densification and rod bending. Uncertainties in nuclear data such as microscopic cross-sections due to measurement errors and deviations in their evaluation model parameters are one of the important sources of computational uncertainties [17].

In this paper, the RMC code and the SCALE 6.2.1 code are used to analyze the sensitivity and uncertainty of nuclear data for the PWR benchmark [18] in the ICSBEP (International Handbook of Evaluated Criticality Safety Benchmark Experiences), and the calculation results of the sensitivity and uncertainty of RMC and SCALE are compared. The IFP method and the superhistory method in the RMC are used to calculate sensitivity. The TSUNAMI-3D-K5 module and the SAMPLER module in the SCALE code system are used to calculate the uncertainty caused by nuclear data.

In the next section, the Monte Carlo method, the first-order uncertainty quantification method, and the stochastic sampling method are introduced. The details of the benchmark are introduced in Section 3. The sensitivity and uncertainty results calculated by the RMC

code and the SCALE code are presented in Section 4. The conclusions are presented in Section 5.

2. Methodology

2.1. Monte Carlo Method

The essence of the Monte Carlo particle transport simulation method is to establish the real movement history of a single particle in a system [19]. The movement history of particles is a random process. The spatial position, initial movement direction, and energy of particles are random variables. Furthermore, the distance from the particle to the next collision point, the type of collision, and the result of the collision are also random processes. The simulation history of a single particle roughly includes the following steps:

1. Stochastically sampling the spatial position, movement direction, and energy generated by particles;
2. Stochastically sampling the distance from the particle to the next collision point, and moving the particle to the collision point;
3. Sampling the collision reaction type. If the particle is not killed (the particle is absorbed or leaves the whole system), the new movement direction and energy are randomly selected according to the reaction type. If secondary particles are generated, they will still be moved using the same method.

There are two main methods to calculate uncertainty by the Monte Carlo method, which are the first-order uncertainty quantification method and the stochastic sampling method.

2.2. The First-Order Uncertainty Quantification Method

The response y can be expressed as a function of the nuclear data $\vec{x} = (x_1, \dots, x_n)$:

$$y = f(x_1, \dots, x_n) \tag{1}$$

Because of the uncertainty of the nuclear data (x_1, \dots, x_n) , the nominal value of the nuclear data is $\vec{x}^0 = (x_1^0, \dots, x_n^0)$, and the error is $(\delta x_1, \dots, \delta x_n)$. Therefore, Equation (1) can be expressed as:

$$y = f(x_1^0 + \delta x_1, \dots, x_n^0 + \delta x_n) \tag{2}$$

The first-order Taylor expansion of response y near the nominal value \vec{x}^0 of the nuclear data is as follows:

$$y = f\left(\vec{x}^0\right) + \sum_{i=1}^n \left(\frac{\partial f}{\partial x_i}\right)_{\vec{x}^0} \delta x_i \tag{3}$$

Suppose the nuclear data (x_1, \dots, x_n) follows the joint probability density function $p(x_1, \dots, x_n)$ [9], then the expected value of this nuclear data is defined as:

$$E(x_i) = x_i^0 \tag{4}$$

$i = 1, \dots, n$, n is the total number of nuclear data. The variance of the nuclear data is defined as:

$$\text{var}(x_i) = \sigma_{x_i}^2 = \int (x_i - x_i^0)^2 p(x_1, \dots, x_n) dx_1 \dots dx_n \tag{5}$$

The covariance of the nuclear data is defined as:

$$\text{cov}(x_i, x_j) = \int (x_i - x_i^0)(x_j - x_j^0) p(x_1, \dots, x_n) dx_1 \dots dx_n \tag{6}$$

The expected value of response y is defined as:

$$E(y) = \sum_{i=1}^n \left(\frac{\partial f}{\partial x_i}\right)_{\vec{x}^0} \int (x_i - x_i^0) p(x_1, \dots, x_n) dx_1 \dots dx_n + f\left(\vec{x}^0\right) = f\left(\vec{x}^0\right) \tag{7}$$

The variance of response y is defined as:

$$\begin{aligned} \text{var}(y) &= \sigma_y^2 = E(y - E(y))^2 = \int \left(\sum_{i=1}^n \left(\frac{\partial f}{\partial x_i} \right)_{\vec{x}=0} \delta x_i \right)^2 p(x_1, \dots, x_n) dx_1 \dots dx_n \\ &= \sum_{i=1}^n \left(\left(\frac{\partial f}{\partial x_i} \right)_{\vec{x}=0} \right)^2 \text{var}(x_i) + 2 \sum_{i=1}^n \left(\frac{\partial f}{\partial x_i} \right)_{\vec{x}=0} \left(\frac{\partial f}{\partial x_j} \right)_{\vec{x}=0} \text{cov}(x_i, x_j) \end{aligned} \quad (8)$$

Equation (8) can be expressed as:

$$\begin{aligned} r_y^2 &= \left(\frac{\sigma_y}{y} \right)^2 = \sum_{i=1}^n \left(\left(\frac{x_i}{y} \frac{\partial f}{\partial x_i} \right)_{\vec{x}=0} \right)^2 \left(\frac{\sigma_{x_i}}{x_i} \right)^2 + 2 \sum_{i \neq j} \left(\frac{x_i}{y} \frac{\partial f}{\partial x_i} \right)_{\vec{x}=0} \left(\frac{x_j}{y} \frac{\partial f}{\partial x_j} \right)_{\vec{x}=0} \frac{\text{cov}(x_i, x_j)}{x_i x_j} \\ &= \sum_{i=1}^n (S_{x_i}^y r_{x_i})^2 + 2 \sum_{i \neq j} S_{x_i}^y S_{x_j}^y r_{\text{cov}}(x_i, x_j) = \vec{S} V_r \vec{S}^T \end{aligned} \quad (9)$$

$S_{x_i}^y = \left(\frac{x_i}{y} \frac{\partial f}{\partial x_i} \right)_{\vec{x}=0}$ is the sensitivity coefficient, $\vec{S} = (S_{x_1}^y, \dots, S_{x_n}^y)$ is the sensitivity coefficient vector, and V_r is the relative covariance matrix corresponding to the nuclear data.

Equation (9) is the sandwich rule. This method can give the uncertainty of the response caused by the uncertainty of each nuclear data, but it depends on the calculation results of the sensitivity coefficients. The sensitivity coefficients are generally obtained by solving the perturbation equation. The more responses there are, the more equations there are to be solved, resulting in a large memory footprint. Therefore, the sandwich rule loses its advantage when there are too many responses. The sensitivity analysis methods in RMC are the IFP method and the superhistory method [20]. The memory footprint of the IFP method is proportional to the number of particles simulated per generation. In the superhistory method, the source perturbation effects are estimated by tracking the source particles and their progenies over super-generations within a single particle history [21]. The memory occupation of the method depends on the expected value of fission neutrons produced by a neutron history rather than being proportional to the number of particles per generation, and thus the method can significantly reduce the memory footprint.

2.3. Stochastic Sampling Method

Figure 1 is the flow chart of the stochastic sampling method. Firstly, samples are randomly sampled based on the uncertainty of nuclear data. Then, for each sample, a Monte Carlo calculation is performed to obtain the calculation results under different samples. Finally, these results are statistically analyzed to calculate the standard deviation of the results, that is, uncertainty. The stochastic sampling method is easy to operate and has strong universality, which is not only applicable to the Monte Carlo code, but also applicable to the deterministic code. In Figure 1, the three responses of k_{eff} , β_{eff} , and λ_{eff} are analyzed simultaneously. However, the stochastic sampling method can only analyze the uncertainty of the calculation results caused by the uncertainty of all parameters at one time. If we want to obtain the uncertainty of the calculation results caused by the uncertainty of a single parameter, we need to perturb each parameter separately and repeat the process shown in Figure 1. For example, in a stochastic sampling calculation, if the ^{235}U and ^{238}U nuclear data are perturbed at the same time, the total uncertainty of the calculation results caused by the uncertainty of the ^{235}U and ^{238}U nuclear data will be obtained. If we want to analyze the uncertainty of the calculation results caused by the uncertainty of the ^{235}U or ^{238}U nuclear data, two stochastic sampling calculations should be conducted, and a single calculation will only perturb one of the ^{235}U and ^{238}U nuclear data.

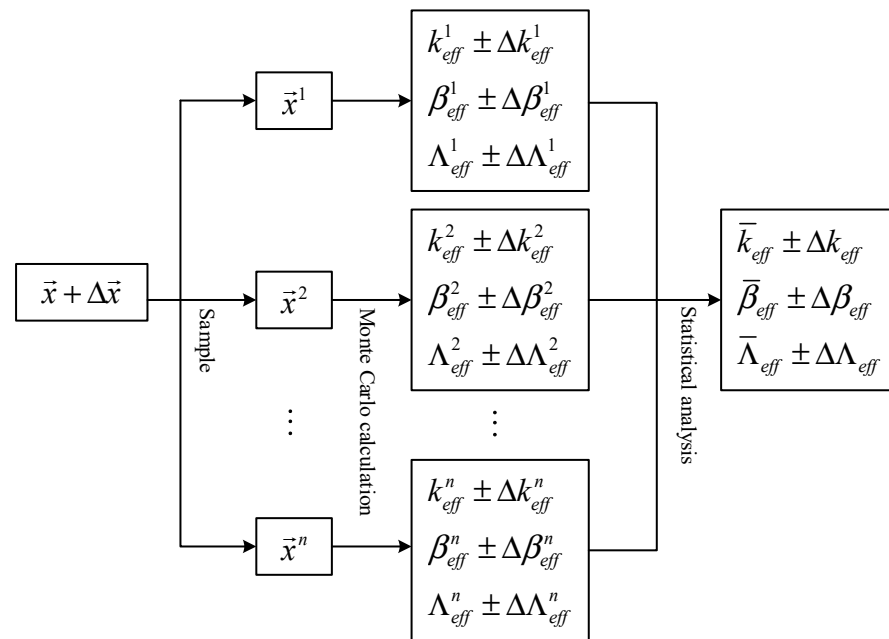


Figure 1. Flow chart of stochastic sampling method.

The selection of sample size depends on the required probability and statistical tolerance limit [22]. The minimum number of samples required can be described by the Wilks equation [23,24]. If the minimum value of samples sampled n times is x_1 and the maximum value is x_n , then the issue is the value of the degree of confidence α when the probability that the sample with an infinite number of samples falls between x_1 and x_n is p . According to the Wilks equation, the relationship between the minimum sample number n , the probability p , and the degree of confidence α is defined as:

$$1 - p^n - n(1 - p)p^{n-1} \geq \alpha \tag{10}$$

The minimum sample number n required for a specific probability p and degree of confidence is shown in Table 1. With a 95% degree of confidence and 95% probability, the minimum number of samples required is 93. Based on the numerical empirical experiment [25], 300 samples are selected for each stochastic sampling calculation, which can not only ensure the calculation accuracy, but also reduce the computation time.

Table 1. Degree of confidence, probability, and sample size.

Degree of Confidence \ Probability	0.90	0.95	0.99
0.90	38	77	388
0.95	46	93	473
0.99	64	130	662

3. Benchmark

B&W’s Core XI conducted a series of low-enrichment UO₂ fuel rod grid experiments at Babcock and Wilcox’s (B&W) Lynchburg Research Center beginning in January 1970 and ending in early 1971. The experiments for Core XI were performed in a large aluminum tank, which was filled with borated water and UO₂ fuel rods. The fuel rods used low-enriched uranium, and the cladding material was aluminum 6061. The water level height was 145 cm, and each loading scheme was slightly supercritical by adjusting the boron concentration in the borated water. In this paper, one eighth of the core of Loading Scheme 8 is chosen to be modeled, and the whole core can be reflected through symmetry, as shown in Figure 2. The core’s central region and a 3 × 3 array of PWR (Pressurized Water Reactor) fuel assemblies are very similar, with fuel rods in each fuel assembly arranged

in a 15×15 lattice. The pitch is 1.6358 cm, and the core diameter is 152.4 cm. The nine assemblies are surrounded by a drive zone consisting of low-enriched uranium fuel rods, which has an irregular boundary. In the entire core of Loading Scheme 8, there are 4808 fuel rods, 9 water holes (located in the center of each fuel assembly), 144 Pyrex rods, no Vicor or Al_2O_3 rods, 794 ppm soluble boron concentration, and 293 K core temperature.

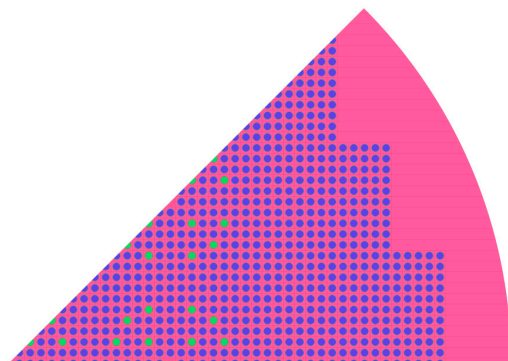


Figure 2. B&W's Core XI 1/8 core.

The Pyrex rod, as shown in Figure 3A, is composed of B, Si, O, Na, and Al materials, with a length of 163.324 cm and a diameter of 1.17 cm. Figure 3B shows the fuel rod. The enrichment of UO_2 is 2.459%. The diameter of the fuel pellet is 1.0297 cm, and the length is 163.324 cm. Al, Mg, Si, Fe, and other materials make up the fuel rod cladding. The cladding thickness is 0.0881 cm. Reference 18 provides more detailed information about the core geometry and materials.

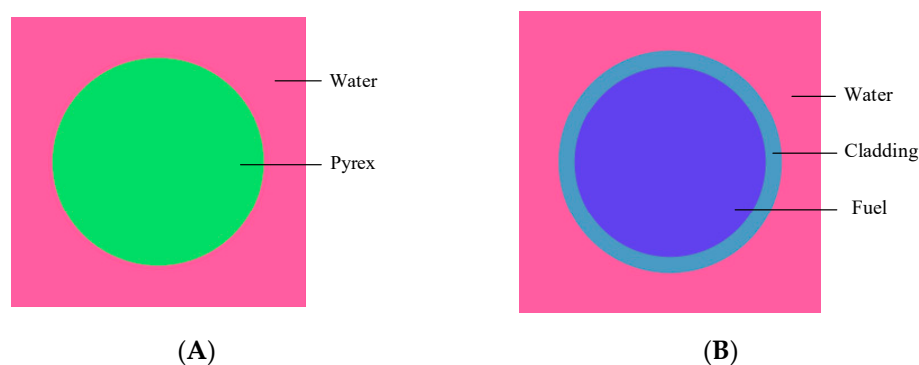


Figure 3. (A) Pyrex Rod, (B) Fuel Rod.

4. Result

4.1. Comparison of Sensitivity

In this paper, TSUNAMI-3D-K5 and RMC are used to calculate the k_{eff} sensitivity to nuclear data for B&W's Core XI Loading Scheme 8. The RMC code uses the ENDF/B-VII.1 library with 500,000 particles, and the SCALE code uses the ENDF/B-VII.0 library and the 238-group ENDF/B-VII.0 library with 200,000 particles. The results of the SCALE code and the RMC code k_{eff} calculation are shown in Table 2, and the relative deviation of the results is -0.087% .

Table 2. SCALE code and RMC code k_{eff} calculation results.

Code	k_{eff}
SCALE	0.997654 ± 0.000099
RMC	0.996782 ± 0.000031

The equation for calculating the relative deviations [26] is defined as:

$$\delta = \frac{x_{RMC} - x_{SCALE}}{x_{SCALE}} \times 100\% \tag{11}$$

In Equation (11), x is one of the SCALE and RMC sensitivity results to a nuclide-reaction type.

The IFP method and the superhistory method of RMC are used to calculate the sensitivity coefficients. The TSUNAMI-3D-K5 module of SCALE is used to calculate the sensitivity coefficients of CE (continuous-energy) and MG (multigroup). As shown in Figure 4, the important nuclear data, primarily ^{235}U fission, ^1H elastic, ^{238}U capture, ^{238}U (n, γ), ^{10}B capture, and ^{10}B (n, α) are in good agreement.

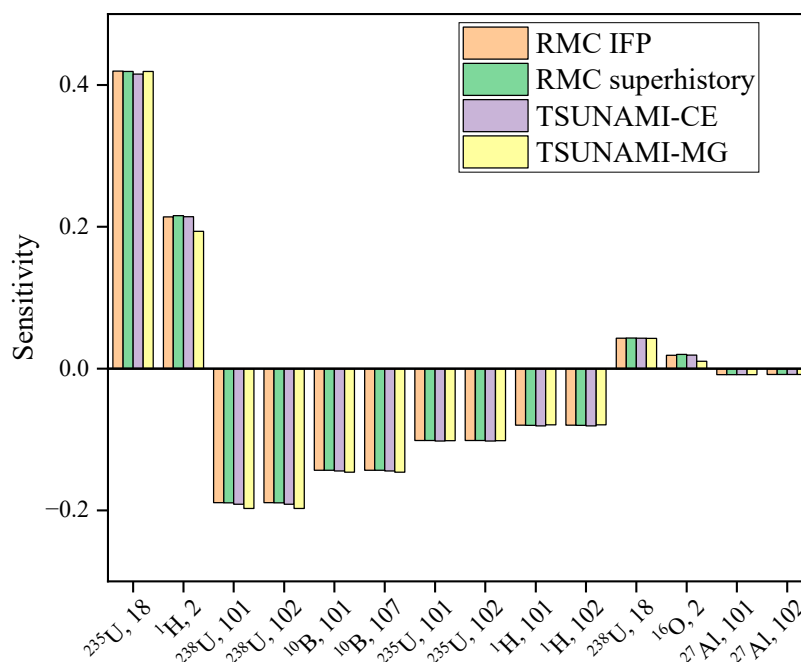


Figure 4. B&W’s Core XI Partial Nuclide Sensitivity.

The reaction types represented by MT numbers used in this paper are shown in Table 3.

Table 3. Reaction type corresponding to MT number.

MT Number	Reaction
2	Elastic scattering
101	Capture
16	($n, 2n$)
18	Fission
102	(n, γ)
103	(n, p)
107	(n, α)
452	$\bar{\nu}$

Table 4 shows the k_{eff} sensitivity results to nuclear data calculated by the SCALE and RMC codes and compares the relative deviations of the results of the two codes.

Table 4. SCALE and RMC code k_{eff} sensitivity to nuclear data.

Nuclide, Reaction Type	Sensitivity			Relative Deviation	
	SCALE	RMC IFP Method	RMC Superhistory Method	SCALE and RMC IFP Method	SCALE and RMC Superhistory Method
^{235}U , fission	$0.4151 \pm 2.049 \times 10^{-4}$	$0.4194 \pm 2.430 \times 10^{-4}$	$0.4189 \pm 8.038 \times 10^{-5}$	1.036%	0.915%
^{235}U , capture	$-0.1022 \pm 3.387 \times 10^{-5}$	$-0.1014 \pm 4.813 \times 10^{-5}$	$-0.1014 \pm 1.457 \times 10^{-5}$	-0.783%	-0.783%
^{235}U , elastic	$8.953 \times 10^{-5} \pm 7.418 \times 10^{-5}$	$-1.197 \times 10^{-6} \pm 9.189 \times 10^{-5}$	$7.887 \times 10^{-5} \pm 3.355 \times 10^{-5}$	-101.337%	-11.907%
^{10}B , capture	$-0.1443 \pm 6.899 \times 10^{-5}$	$-0.1435 \pm 9.588 \times 10^{-5}$	$-0.1435 \pm 3.193 \times 10^{-5}$	-0.554%	-0.554%
^{10}B , (n, α)	$-0.1443 \pm 6.898 \times 10^{-5}$	$-0.1434 \pm 9.587 \times 10^{-5}$	$-0.1435 \pm 3.192 \times 10^{-5}$	-0.624%	-0.554%
^{238}U , capture	$-0.1912 \pm 7.072 \times 10^{-5}$	$-0.1892 \pm 1.108 \times 10^{-4}$	$-0.1893 \pm 3.222 \times 10^{-5}$	-1.046%	-0.994%
^{238}U , (n, γ)	$-0.1911 \pm 7.068 \times 10^{-5}$	$-0.1892 \pm 1.108 \times 10^{-4}$	$-0.1893 \pm 3.222 \times 10^{-5}$	-0.994%	-0.942%
^{238}U , (n, 2n)	$1.229 \times 10^{-3} \pm 6.963 \times 10^{-6}$	$9.965 \times 10^{-4} \pm 1.932 \times 10^{-5}$	$9.974 \times 10^{-4} \pm 9.482 \times 10^{-6}$	-18.918%	-18.845%
^1H , elastic	$0.2142 \pm 1.671 \times 10^{-3}$	$0.2138 \pm 2.063 \times 10^{-3}$	$0.2157 \pm 6.569 \times 10^{-4}$	-0.187%	0.700%
^1H , (n, γ)	$-8.075 \times 10^{-2} \pm 3.135 \times 10^{-5}$	$-7.994 \times 10^{-2} \pm 4.478 \times 10^{-5}$	$-7.999 \times 10^{-2} \pm 1.422 \times 10^{-5}$	-1.003%	-0.941%
^{16}O , elastic	$1.899 \times 10^{-2} \pm 6.586 \times 10^{-4}$	$1.884 \times 10^{-2} \pm 9.363 \times 10^{-4}$	$1.994 \times 10^{-2} \pm 2.902 \times 10^{-4}$	-0.790%	5.003%
^{16}O , (n, α)	$-2.889 \times 10^{-3} \pm 4.474 \times 10^{-4}$	$-2.875 \times 10^{-3} \pm 6.655 \times 10^{-6}$	$-2.870 \times 10^{-3} \pm 1.996 \times 10^{-6}$	-0.485%	-0.658%

From Table 3, it can be seen that most of the calculations of the SCALE and RMC procedures are in good agreement, and the elastic scattering reaction type of ^{235}U and the (n,2n) reaction type of ^{238}U are in poor agreement. Table 5 shows the standard deviation calculated by SCALE and RMC for the two nuclides. The equation for calculating the relative combined standard deviation [26] is defined as:

$$\text{STD} = \sqrt{(\text{STD}_{\text{RMC}})^2 + (\text{STD}_{\text{SCALE}})^2} \quad (12)$$

Table 5. Standard deviation of some nuclides reaction types.

Nuclide, Reaction Type	Standard Deviation			Relative Combined Standard Deviation	
	SCALE	RMC IFP Method	RMC Superhistory Method	SCALE and RMC IFP Method	SCALE and RMC Superhistory Method
^{235}U , elastic	7.418×10^{-5}	9.189×10^{-5}	3.355×10^{-5}	1.181×10^{-4}	8.141×10^{-5}
^{238}U , (n, 2n)	6.963×10^{-6}	1.932×10^{-5}	9.482×10^{-6}	2.152×10^{-5}	1.176×10^{-5}

In Equation (12), STD_{RMC} is the standard deviation of k_{eff} sensitivity to nuclear data calculated by the RMC code.

The sensitivity calculation results of the RMC code for the elastic scattering reaction type of ^{235}U in Table 4 are within three times the relative combined standard deviation of the calculation results of the SCALE code. That is, the sensitivity calculation of the RMC code satisfies both the conditions of the sensitivity calculation results being greater than the SCALE code minus three times the relative combined standard deviation, and being less than the sensitivity calculation results of the SCALE code plus three times the relative combined standard deviation. However, the results of the two codes for the ^{238}U (n, 2n) reaction type are in poor agreement, and the sensitivity calculation results of the RMC code are not within three times the relative combined standard deviation of the SCALE calculation results.

The IFP method and superhistory method in the RMC code are used calculate the k_{eff} sensitivity to nuclear data, both of which have 500,000 particles, 100 inactive generations, and 900 active generations, with 50 cores in parallel. As shown in Table 6, although the IFP method can save about half of the running time, the memory footprint is more than 20 times that of the superhistory method. The more nuclides and reaction types that are analyzed, the more memory is required. It is difficult for general-purpose equipment to meet such a large memory demand. For this situation, the superhistory method has obvious advantages.

Table 6. Performance of the IFP method and the superhistory method in RMC.

Method	Memory Footprint/G	Running Time/Minutes
IFP method	About 180	541
Superhistory method	About 8	1150

4.2. Comparison of Uncertainty

4.2.1. SCALE 56-Group-cov7.1 Covariance Library

TSUNAMI-CE, TSUNAMI-MG, and RMC are used to calculate the uncertainty in k_{eff} caused by the nuclear data uncertainty of the PWR benchmark. The RMC code uses the 44-group covariance library in the SCALE6.1 code, and the SCALE code uses the 56-group-cov7.1 covariance library. The uncertainty calculation of TSUNAMI and RMC uses the first-order uncertainty quantification method, and the uncertainty calculation results are shown in Figure 5.

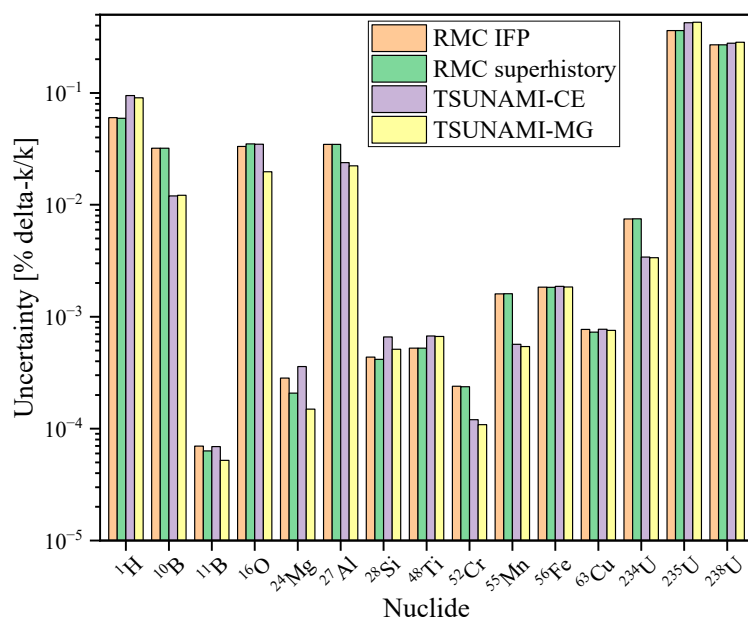


Figure 5. Uncertainty in k_{eff} caused by uncertainty of nuclear data of different nuclides (SCALE 56-group-cov7.1 covariance library).

It can be seen from Figure 5 that the uncertainty of the ^{235}U and ^{238}U nuclear data contributes the most to the uncertainty in k_{eff} , and the calculation results are in good agreement. The uncertainty calculation results for each nuclide are shown in Table 7. The RMC value in the table is the average value of the IFP method and the superhistory method, and the TSUNAMI value is the average value of CE and MG.

The relative deviations of ^{10}B , ^{52}Cr , ^{55}Mn , and ^{234}U in Table 7 exceed 100%. Comparing the sensitivity values of these nuclides, as shown in Table 8, the sensitivity results calculated by the two codes are in good agreement. The uncertainties of these four nuclides are calculated by the first-order uncertainty quantification method, which is closely related to the sensitivity and covariance library. Therefore, the reason for the large relative deviation between the two codes should be the use of a different covariance library.

Table 7. Uncertainty of nuclides (SCALE 56-group-cov7.1 covariance library).

Nuclide	RMC [% δ -k/k]	TSUNAMI [% δ -k/k]	Relative Deviation
H-1	$5.983 \times 10^{-2} \pm 3.075 \times 10^{-5}$	$9.247 \times 10^{-2} \pm 5.053 \times 10^{-6}$	−35.303%
B-10	$3.201 \times 10^{-2} \pm 3.858 \times 10^{-7}$	$1.210 \times 10^{-2} \pm 2.771 \times 10^{-8}$	164.545%
B-11	$6.650 \times 10^{-5} \pm 1.650 \times 10^{-9}$	$6.065 \times 10^{-5} \pm 1.480 \times 10^{-9}$	9.653%
O-16	$3.412 \times 10^{-2} \pm 3.519 \times 10^{-5}$	$2.728 \times 10^{-2} \pm 3.582 \times 10^{-5}$	25.073%
Mg-24	$2.457 \times 10^{-4} \pm 1.533 \times 10^{-7}$	$2.542 \times 10^{-4} \pm 4.150 \times 10^{-8}$	−3.329%
Al-27	$3.469 \times 10^{-2} \pm 7.283 \times 10^{-6}$	$2.313 \times 10^{-2} \pm 9.836 \times 10^{-6}$	49.978%
Si-28	$4.267 \times 10^{-4} \pm 1.849 \times 10^{-8}$	$5.863 \times 10^{-4} \pm 9.169 \times 10^{-8}$	−27.223%
Ti-48	$5.246 \times 10^{-4} \pm 2.494 \times 10^{-9}$	$6.708 \times 10^{-4} \pm 2.754 \times 10^{-9}$	−21.799%
Cr-52	$2.388 \times 10^{-4} \pm 5.713 \times 10^{-9}$	$1.144 \times 10^{-4} \pm 3.850 \times 10^{-9}$	108.666%
Mn-55	$1.605 \times 10^{-3} \pm 4.055 \times 10^{-8}$	$5.548 \times 10^{-4} \pm 3.268 \times 10^{-8}$	189.299%
Fe-56	$1.835 \times 10^{-3} \pm 1.797 \times 10^{-8}$	$1.855 \times 10^{-3} \pm 1.876 \times 10^{-8}$	−1.078%
Cu-63	$7.508 \times 10^{-4} \pm 3.135 \times 10^{-8}$	$7.648 \times 10^{-4} \pm 1.399 \times 10^{-8}$	−1.827%
U-234	$7.495 \times 10^{-3} \pm 7.169 \times 10^{-7}$	$3.395 \times 10^{-3} \pm 4.892 \times 10^{-8}$	120.766%
U-235	$0.3607 \pm 3.241 \times 10^{-5}$	$0.4257 \pm 2.788 \times 10^{-5}$	−15.270%
U-238	$0.2696 \pm 2.671 \times 10^{-4}$	$0.2808 \pm 4.185 \times 10^{-5}$	−3.978%

Table 8. Sensitivity of total reaction type.

Nuclide, Reaction Type	RMC	TSUNAMI	Relative Deviation
^{10}B , total	$-0.1435 \pm 9.477 \times 10^{-5}$	$-0.1453 \pm 7.032 \times 10^{-5}$	−1.239%
^{52}Cr , total	$-2.473 \times 10^{-5} \pm 1.265 \times 10^{-5}$	$-2.373 \times 10^{-5} \pm 8.829 \times 10^{-6}$	4.210%
^{55}Mn , total	$-3.832 \times 10^{-4} \pm 2.788 \times 10^{-5}$	$-3.910 \times 10^{-4} \pm 1.960 \times 10^{-5}$	−1.996%
^{234}U , total	$-1.389 \times 10^{-3} \pm 1.197 \times 10^{-5}$	$-1.387 \times 10^{-3} \pm 8.750 \times 10^{-6}$	0.202%

4.2.2. SCALE 44-Group Covariance Library

The 56-group-cov7.1 covariance library used in the SCALE code is changed to the 44-group covariance library and recalculated, and the results are shown in Figure 6. It can be seen from Figure 6 that the uncertainty of the ^{235}U and ^{238}U nuclear data contributes the most to the uncertainty in k_{eff} , and the calculation results are also in good agreement.

The uncertainty calculation results for each nuclide and relative deviations are shown in Table 9. The RMC value in the table is the average value of the IFP method and the superhistory method, and the TSUNAMI value is the average value of CE and MG.

The degree of uncertainty agreement is significantly improved when the same covariance library is used for both codes. This shows that the large relative deviation between the two codes in Table 7 is caused by different covariance libraries.

The uncertainties of the partial reaction pairs for the different nuclides are shown in Figure 7, and both RMC and SCALE are calculated using the 44-group covariance library. The results of the RMC IFP method and the superhistory method are in good agreement. The TSUNAMI-CE and TSUNAMI-MG results are mostly in good agreement, with some reaction pairs in poor agreement. The relative deviations of different codes for large uncertainty results are small.

The SAMPLER module in SCALE is used to calculate the uncertainty in k_{eff} . Only the cross-sections are perturbed, with 300 stochastic samples. Using generic regular expressions (GREP), the k_{eff} calculation result is extracted to obtain the total uncertainty. Table 10 shows the total uncertainty calculated by the first-order uncertainty quantification method and the stochastic sampling method. The total uncertainty calculated using the first-order uncertainty quantification method is in good agreement for both codes. Among them, the difference between the uncertainty in the k_{eff} results of TSUNAMI-MG and RMC is the largest, and their relative deviation is −2.615%. The maximum relative deviation of the total uncertainty calculated by the first-order uncertainty quantification method and the stochastic sampling method is 8.53%.

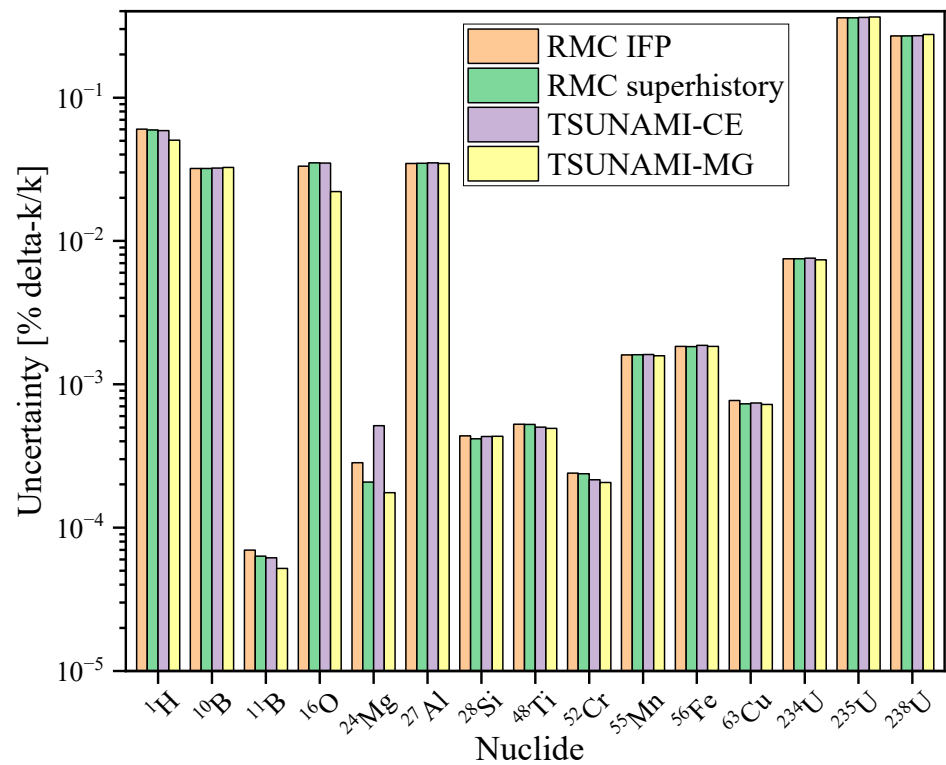
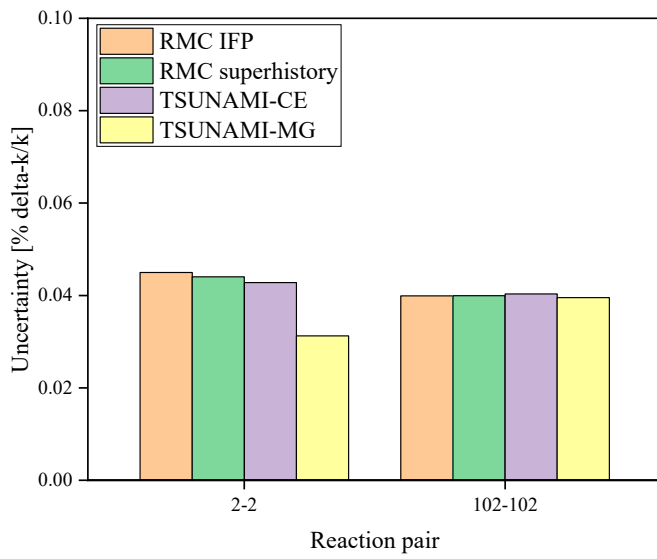


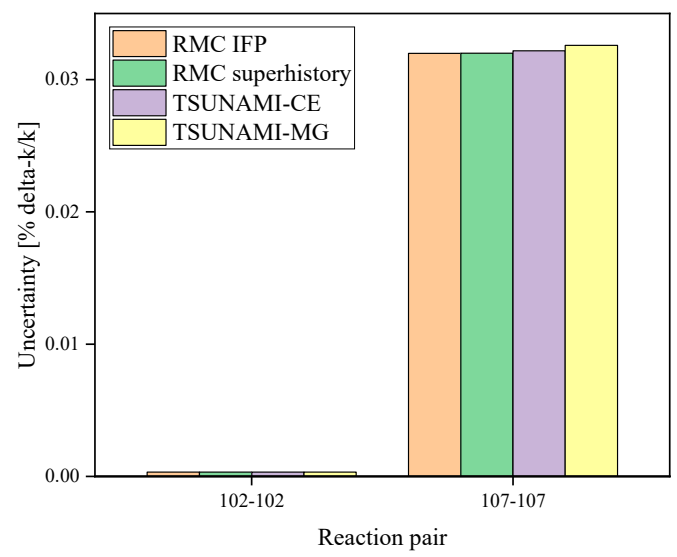
Figure 6. Uncertainty in k_{eff} caused by uncertainty of nuclear data of different nuclides (SCALE 44-group covariance library).

Table 9. Uncertainty of nuclides (SCALE 44-group covariance library).

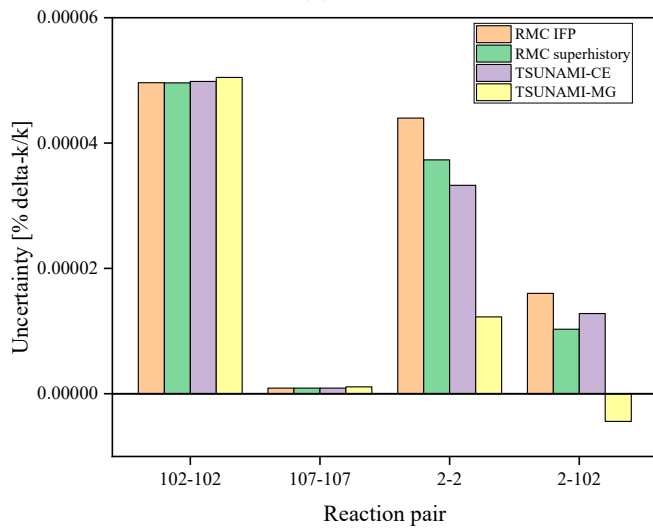
Nuclide	RMC [%delta-k/k]	TSUNAMI [%delta-k/k]	Relative Deviation
H-1	$5.983 \times 10^{-2} \pm 3.075 \times 10^{-5}$	$5.461 \times 10^{-2} \pm 2.036 \times 10^{-5}$	9.542%
B-10	$3.201 \times 10^{-2} \pm 3.858 \times 10^{-7}$	$3.240 \times 10^{-2} \pm 2.474 \times 10^{-7}$	−1.204%
B-11	$6.650 \times 10^{-5} \pm 1.650 \times 10^{-9}$	$5.684 \times 10^{-5} \pm 1.759 \times 10^{-9}$	16.988%
O-16	$3.412 \times 10^{-2} \pm 3.519 \times 10^{-5}$	$2.846 \times 10^{-2} \pm 2.600 \times 10^{-5}$	19.904%
Mg-24	$2.457 \times 10^{-4} \pm 1.533 \times 10^{-7}$	$3.455 \times 10^{-4} \pm 1.453 \times 10^{-7}$	−28.874%
Al-27	$3.469 \times 10^{-2} \pm 7.283 \times 10^{-6}$	$3.486 \times 10^{-2} \pm 5.100 \times 10^{-6}$	−0.479%
Si-28	$4.267 \times 10^{-4} \pm 1.849 \times 10^{-8}$	$4.332 \times 10^{-4} \pm 1.241 \times 10^{-8}$	−1.512%
Ti-48	$5.246 \times 10^{-4} \pm 2.494 \times 10^{-9}$	$4.973 \times 10^{-4} \pm 2.119 \times 10^{-9}$	5.493%
Cr-52	$2.388 \times 10^{-4} \pm 5.713 \times 10^{-9}$	$2.112 \times 10^{-4} \pm 2.718 \times 10^{-9}$	13.074%
Mn-55	$1.605 \times 10^{-3} \pm 4.055 \times 10^{-8}$	$1.595 \times 10^{-3} \pm 6.420 \times 10^{-8}$	0.651%
Fe-56	$1.835 \times 10^{-3} \pm 1.797 \times 10^{-8}$	$1.855 \times 10^{-3} \pm 1.038 \times 10^{-8}$	−1.023%
Cu-63	$7.508 \times 10^{-4} \pm 3.135 \times 10^{-8}$	$7.306 \times 10^{-4} \pm 1.430 \times 10^{-8}$	2.774%
U-234	$7.495 \times 10^{-3} \pm 7.169 \times 10^{-7}$	$7.491 \times 10^{-3} \pm 4.186 \times 10^{-7}$	0.071%
U-235	$0.3607 \pm 3.241 \times 10^{-5}$	$3.634 \pm 1.083 \times 10^{-4}$	−0.752%
U-238	$0.2696 \pm 2.671 \times 10^{-4}$	$2.727 \pm 1.713 \times 10^{-4}$	−1.143%



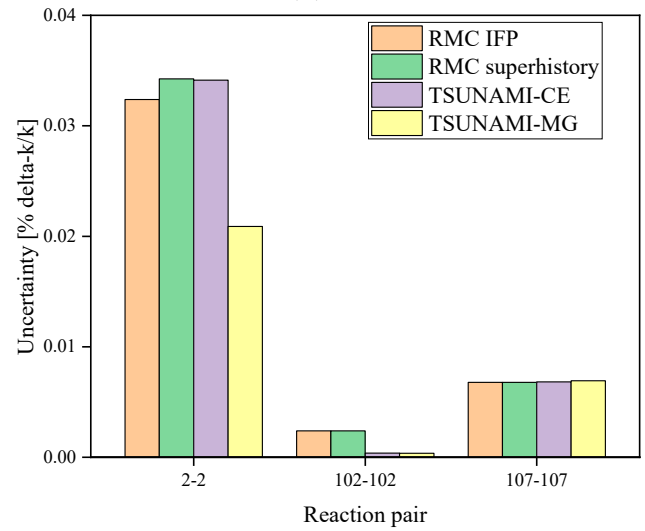
(a) ^1H



(b) ^{10}B

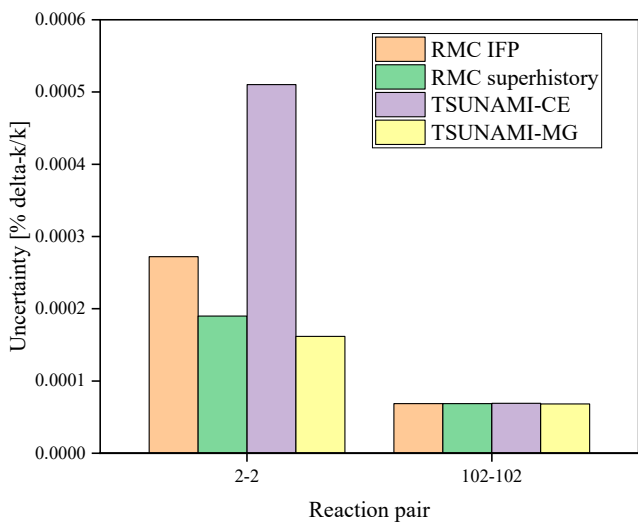


(c) ^{11}B

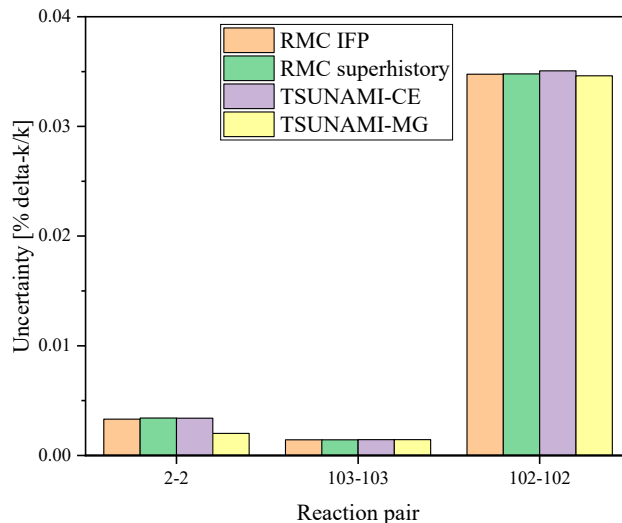


(d) ^{16}O

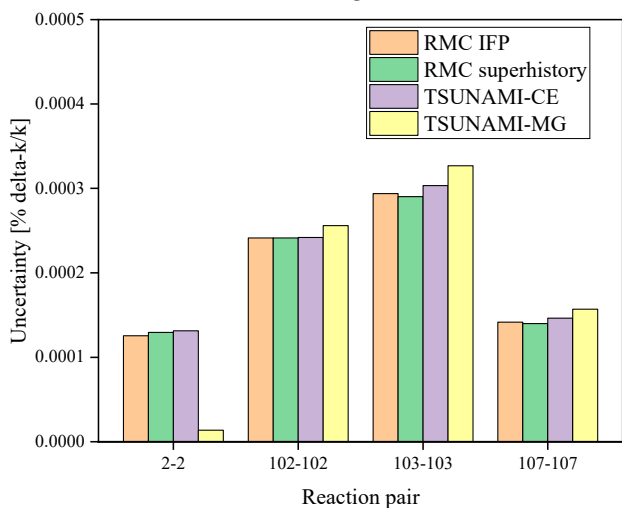
Figure 7. Cont.



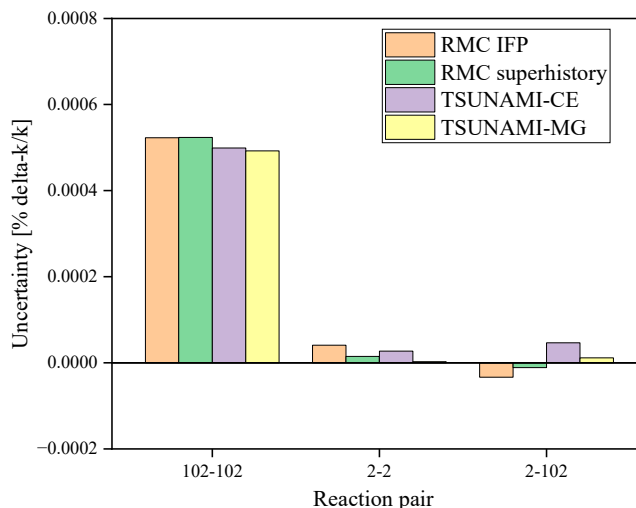
(e) ^{24}Mg



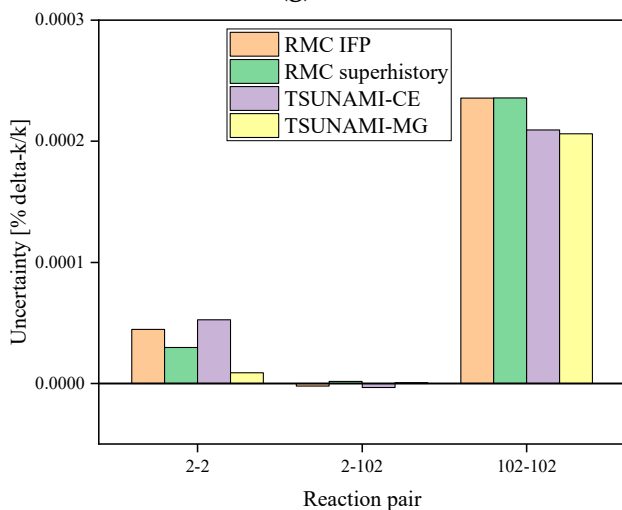
(f) ^{27}Al



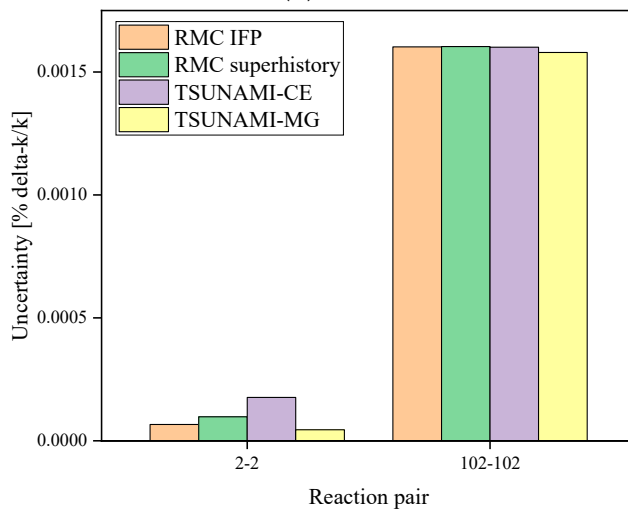
(g) ^{28}Si



(h) ^{48}Ti

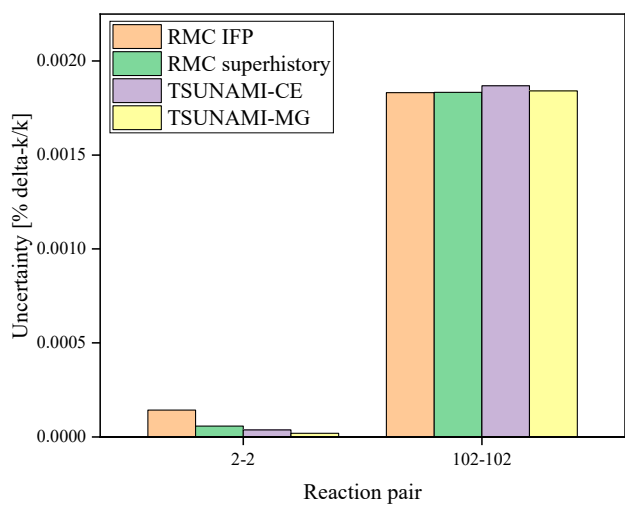


(i) ^{52}Cr

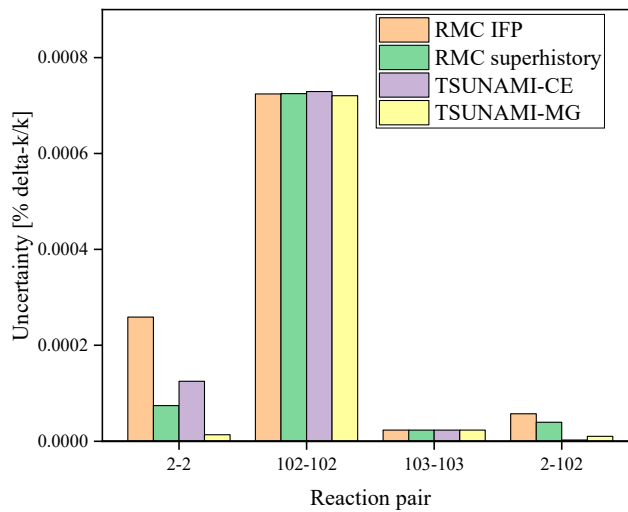


(j) ^{55}Mn

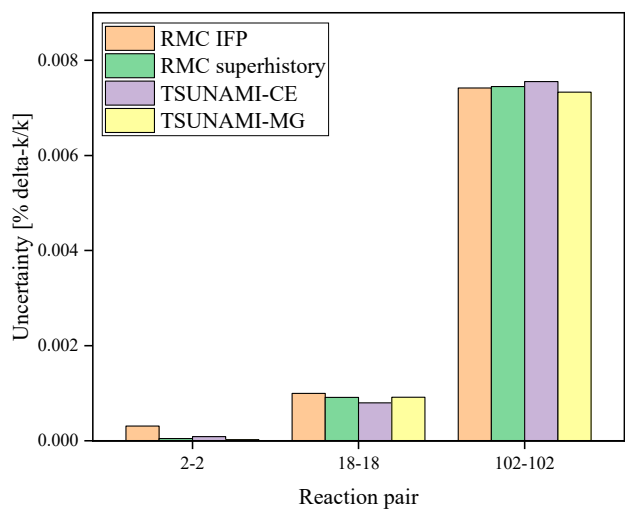
Figure 7. Cont.



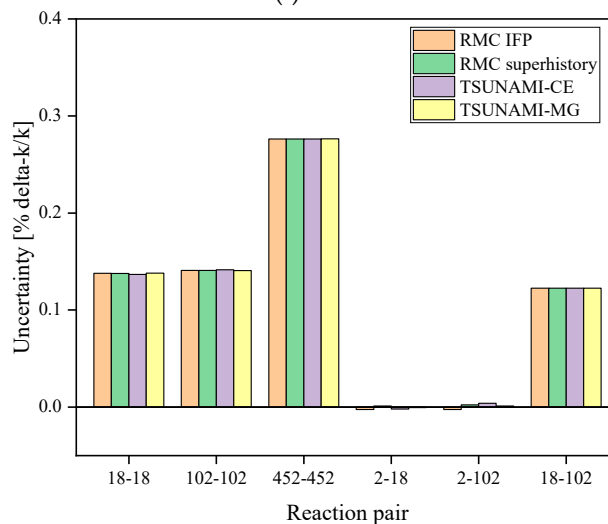
(k) ^{56}Fe



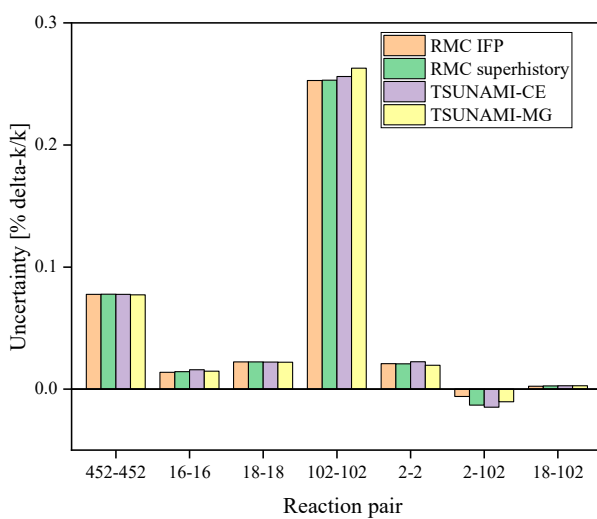
(l) ^{63}Cu



(m) ^{234}U



(n) ^{235}U



(o) ^{238}U

Figure 7. Uncertainty of partial reaction pairs of different nuclides.

Table 10. Total uncertainty in k_{eff} .

Code	TSUNAMI-CE	TSUNAMI-MG	RMC	SAMPLER
Uncertainty [% $\Delta k/k$]	0.4596	0.4627	0.4506	0.4926

5. Conclusions

In this work, the B&W's Core XI benchmark was modeled using RMC and SCALE to verify the accuracy of the sensitivity and uncertainty analysis methods developed in RMC. The sensitivity and uncertainty calculation results of the IFP method and the superhistory method of RMC were compared with that of TSUNAMI-CE/MG in SCALE. The nuclear cross-sections with high sensitivity and the uncertainty of nuclides with large contributions to the uncertainty in k_{eff} were in good agreement between the two codes. Verification shows that the capabilities of sensitivity and uncertainty analysis developed in the RMC code has good accuracy.

A detailed comparative analysis of the advantages and disadvantages of different sensitivity and uncertainty analysis methods was also conducted. The total uncertainty in the k_{eff} of the first-order uncertainty quantification method was compared with that of the stochastic sampling method, and the maximum relative deviation of total uncertainties in k_{eff} is 8.53%. Moreover, compared with the IFP method, the superhistory method can reduce the memory footprint by more than 95%, but the computation time was only about twice as much as the IFP method. The superhistory method shows advantages for the cases which have many nuclides and reaction types to be analyzed.

Author Contributions: Conceptualization, S.L. and C.J.; methodology, S.L.; software, J.L.; validation, C.J. and S.Z.; formal analysis, C.J.; investigation, C.J.; writing—original draft preparation, C.J. and S.Z.; writing—review and editing, Y.C. and S.Z.; funding acquisition, S.L. All authors have read and agreed to the published version of the manuscript.

Funding: This research was funded by Project 12175067/11905060 of the National Natural Science Foundation of China, the Natural Science Foundation of Hebei Province (no. A2022502008), the Fundamental Research Funds for the Central Universities (2022JG002), and the Young Elite Scientists Sponsorship Program (2020QNRC001) of China Association for Science and Technology.

Data Availability Statement: Not applicable.

Conflicts of Interest: The authors declare no conflict of interest.

References

- Chersola, D.; Mazzini, G.; Košťál, M.; Miglierini, B.; Hrehor, M.; Lomonaco, G.; Borreani, W.; Ruščák, M. Application of Serpent 2 and MCNP6 to study different criticality configurations of a VVER-1000 mock-up. *Ann. Nucl. Energy* **2016**, *94*, 109–122. [\[CrossRef\]](#)
- Liu, S.; Wang, G.; Liang, J.; Wu, G.; Wang, K. Burnup-dependent core neutronics analysis of plate-type research reactor using deterministic and stochastic methods. *Ann. Nucl. Energy* **2015**, *85*, 830–836. [\[CrossRef\]](#)
- Liu, S.; Wang, G.; Wu, G.; Wang, K. Neutronics comparative analysis of plate-type research reactor using deterministic and stochastic methods. *Ann. Nucl. Energy* **2015**, *79*, 133–142. [\[CrossRef\]](#)
- Kelly, D.J., III; Kelly, A.E.; Aviles, B.N.; Godfrey, A.T.; Salko, R.K.; Collins, B.S. MC21/CTF and VERA multiphysics solutions to VERA core physics benchmark progression problems 6 and 7. *Nucl. Eng. Technol.* **2017**, *49*, 1326–1338. [\[CrossRef\]](#)
- Leppänen, J.; Mattila, R.; Pusa, M. Validation of the Serpent-ARES code sequence using the MIT BEAVRS benchmark—Initial core at HZP conditions. *Ann. Nucl. Energy* **2014**, *69*, 212–225. [\[CrossRef\]](#)
- Goorley, T.; James, M.; Booth, T.; Brown, F.; Bull, J.; Cox, L.J.; Durkee, J.; Elson, J.; Fensin, M.; Forster, R.A.; et al. Initial MCNP6 Release Overview. *Nucl. Technol.* **2012**, *180*, 298–315. [\[CrossRef\]](#)
- Rearden, B.T.; Williams, M.L.; Jessee, M.A.; Mueller, D.E.; Wiarda, D.A. Sensitivity and uncertainty analysis capabilities and data in SCALE. *Nucl. Technol.* **2011**, *174*, 236–288. [\[CrossRef\]](#)
- Baker, C.; Smith, P.N.; Mason, R.; Shepherd, M.; Richards, S.; Hiles, R.; Perry, R.; Hanlon, D.; Dobson, G. Calculating Uncertainty on K-effective with MONK10. In Proceedings of the ICNC 2015, Anaheim, CA, USA, 16–19 February 2015; pp. 1073–1082.
- Aufiero, M.; Bidaud, A.; Hursin, M.; Leppänen, J.; Palmiotti, G.; Pelloni, S.; Rubiolo, P. A collision history-based approach to sensitivity/perturbation calculations in the continuous energy Monte Carlo code SERPENT. *Ann. Nucl. Energy* **2015**, *85*, 245–258. [\[CrossRef\]](#)

10. Wang, K.; Li, Z.; She, D.; Liang, J.; Xu, Q.; Qiu, Y.; Yu, J.; Sun, J.; Fan, X.; Yu, G. RMC—A Monte Carlo code for reactor core analysis. *Ann. Nucl. Energy* **2015**, *82*, 121–129. [[CrossRef](#)]
11. Liu, S.; Yuan, Y.; Yu, J.; Wang, K. Development of on-the-fly temperature-dependent cross-sections treatment in RMC code. *Ann. Nucl. Energy* **2016**, *94*, 144–149. [[CrossRef](#)]
12. Saylor, E.M.; Marshall, W.J.; Clarity, J.B.; Clifton, Z.J.; Rearden, B.T. *Criticality Safety Validation of SCALE 6.2.2*; Technical Report ORNL/TM-2018/884; Oak Ridge National Laboratory: Oak Ridge, TN, USA, 2018.
13. Perfetti, C.M.; Rearden, B.T. Development of a Generalized Perturbation Theory Method for Sensitivity Analysis Using Continuous-Energy Monte Carlo Methods. *Nucl. Sci. Eng.* **2016**, *182*, 354–368. [[CrossRef](#)]
14. Cacuci, D.G. *Handbook of Nuclear Engineering*; Nuclear Engineering Fundamentals; Springer: Berlin/Heidelberg, Germany, 2010; Volume I.
15. Qiu, Y.S. *Nuclear Data Sensitivity and Uncertainty Analysis in the Burnup Calculation Based on RMC Code*; Tsinghua University: Beijing, China, 2017.
16. Shi, G.; Jia, C.; Guo, X.; Li, K.; Wang, K.; Huang, S.; Cheng, Q. Improved generalized perturbation theory method for sensitivity analysis of generalized response function. *Prog. Nucl. Energy* **2021**, *134*, 103643. [[CrossRef](#)]
17. Ware, T.; Dobson, G.; Hanlon, D.; Hiles, R.; Mason, R.; Perry, R. Determining the nuclear data uncertainty on MONK10 and WIMS10 criticality calculations. *EPJ Web Conf.* **2017**, *146*, 06023. [[CrossRef](#)]
18. Mosteller, R.D.; Pelowitz, D.B. *Critical Lattices of UO₂ Fuel Rods and Perturbing Rods in Borated Water*; Nuclear Energy Agency: Paris, France, 1995; Report NEA/NSC/DOC(95)03/IV; Volume IV LEU-COMP-THERM-008.
19. Haghghat, A. *Monte Carlo Methods for Particle Transport*; CRC Press: Boca Raton, FL, USA, 2020.
20. Qiu, Y.; Shang, X.; Tang, X.; Liang, J.; Wang, K. Computing eigenvalue sensitivity coefficients to nuclear data by adjoint superhistory method and adjoint Wielandt method implemented in RMC code. *Ann. Nucl. Energy* **2016**, *87*, 228–241. [[CrossRef](#)]
21. Shi, G.; Yu, G.; Jia, C.; Wang, K.; Huang, S.; Cheng, Q.; Li, H. Superhistory-based differential operator method for generalized responses sensitivity calculations. *Ann. Nucl. Energy* **2020**, *140*, 107291. [[CrossRef](#)]
22. Glaeser, H. GRS Method for Uncertainty and Sensitivity Evaluation of Code Results and Applications. *Sci. Technol. Nucl. Install.* **2008**, *2008*, 1–7. [[CrossRef](#)]
23. Wilks, S.S. Determination of Sample Sizes for Setting Tolerance Limits. *Ann. Math. Stat.* **1941**, *12*, 91–96. [[CrossRef](#)]
24. Wilks, S.S. Statistical Prediction with Special Reference to the Problem of Tolerance Limits. *Ann. Math. Stat.* **1942**, *13*, 400–409. [[CrossRef](#)]
25. Rochman, D.; Zwermann, W.; van der Marck, S.C.; Koning, A.J.; Sjöstrand, H.; Helgesson, P.; Krzykacz-Hausmann, B. Efficient use of Monte Carlo: Uncertainty propagation. *Nucl. Sci. Eng.* **2014**, *177*, 337–349. [[CrossRef](#)]
26. Zhang, X.; Liu, S.; Yan, Y.; Qin, Y.; Chen, Y. Application of the neutron-photon-electron coupling transport of cosRMC in fusion neutronics. *Fusion Eng. Des.* **2020**, *159*, 111875. [[CrossRef](#)]